Vibration Study of Clamped-Free Elliptical Cylindrical Shells

JOHN L. SEWALL* AND CHRISTINE G. PUSEY†
NASA Langley Research Center, Hampton, Va.

This paper reports an experimental and analytical vibration study of elliptical cylindrical shells having a wide range of cross-sectional eccentricities. Vibration tests were conducted on four thin-shell, isotropic, clamped-free cylinders of equal length, perimeter, and thickness with eccentricities ranging from zero (circular cylinder) to 0.916, corresponding to major-to-minor axis ratios from 1 to 2.5, respectively. Mode shapes were obtained through the use of a noncontact, inductance-type proximity sensor that could be moved automatically over the shell surface. Measured frequencies and mode shapes are compared with analytical frequencies and mode shapes obtained by application of a Rayleigh-Ritz type of vibration analysis featuring multiterm circumferential and longitudinal modal expansions. Results show generally good agreement between experiment and analysis. Reductions in frequency by as much as 44% were found for an eccentricity of 0.916.

Nomenclature

a,b	=	length of major and minor semiaxes, respectively, of elliptical cylindrical shell
E	=	Young's modulus
e	=	$[1 - (b/a)^2]^{1/2}$ = eccentricity of elliptical cylindrical shell
f	=	circular frequency, Hz
L	=	length of shell
m	=	longitudinal mode numbers
N_m	=	beam-function eigenvalue [see Eq. (2)]
n	=	number of circumferential waves for circular cylindrical shell
P,Q	=	integers identifying upper limits on number of modal functions used in analysis [see Eq. (1)]
p	=	circumferential wave number denoting half the number of longitudinal node lines for elliptical cylindrical shell
R	=	radius of curvature of shell
s	=	arc length of shell cross section
s_0	=	total circumference of shell cross section
u,v,w	=	longitudinal, circumferential, and radial (or normal) shell displacements, respectively (see Fig. 5)
X_{mu},X_{mv},X_{mw}	=	mth longitudinal mode shapes for u, v, and w displacements, respectively
x,y,z	=	longitudinal and cross-sectional coordinates of an elliptical shell (see Fig. 5)
γ_m	=	beam-function eigenvalue property [see Eq. (2)]
θ	=	angle between minor axis of elliptical cross section and radius vector R (see Fig. 5)
μ	=	Poisson's ratio
ρ	=	shell mass density
ϕ	=	central angle (see Fig. 5)
ω	=	angular frequency, rad/sec

Subscripts

m	=	identifies mth longitudinal modal component
p	=	identifies pth circumferential modal component

Introduction

IN any review of the literature on shell dynamics, it is readily apparent that structural dynamicists have been more concerned with shells of revolution than with noncircular shells. This emphasis is certainly understandable in view of the many aerospace and submarine components that can be adequately treated as actual or equivalent shells of revolution. However, the existence of cylindrical shell elements whose curvature is significantly noncircular has evidently been sufficient to motivate the investigations reported[1–11] on the dynamic characteristics of these elements. In a number of these writings,[2–5] the radius of curvature is represented by Fourier-series types of approximations that are functions of the cross-sectional eccentricity. Other investigators have used the actual radius of curvature of an elliptical shell in structural studies of this cross-sectionl shape.[6,7,9] Most of these studies are entirely analytical with little or no experimental data included for comparison with analytical results. Experimental frequencies and mode shapes are given in two of these studies.[9,10] Data are given in Ref. 9 for both unstiffened and ring- and stringer-stiffened clamped-free elliptical cylindrical shells, all having the same cross-sectional eccentricity.

The purposes of the present paper are 1) to compare measured with analytical frequencies and mode shapes of a family of elliptical cylindrical shells of constant mass, clamped at one end and free at the other, and 2) to determine the effects of cross-sectional eccentricity on these vibration data The paper reports a portion of a larger research program[11] which includes a vibration study of free-free elliptical cylinders. Vibration tests were conducted on four short thin-shell isotropic cylinders with eccentricities ranging from zero (circular cylinder) to 0.916 and corresponding to major-to-minor axis ratios from 1 to 2.5, respectively. Frequencies and mode shapes were measured for a large number of resonances observed for each model. Analytical frequencies and mode shapes were calculated by application of a Rayleigh-Ritz analysis involving multiterm circumferential and longitudinal modal expansions.[11] Trigonometric functions were chosen for the circumferential series, and elementary beam vibration functions for the longitudinal (or axial) series. The actual elliptical radius of curvature was used.

Experimental Investigation

Models

Four cylindrical-shell models were used in the vibration tests, one of circular and three of elliptical cross section. Each model was 24 in. long and was made from two shaped sections, each of 6061 aluminum alloy, 0.032 in. thick, and butt-welded together with smoothed seams at the ends of the major axis. The perimeter, length, and thickness were each held fixed so as to make the total mass constant for all models.

Received July 15, 1970; revision received January 18, 1971. The authors herewith express their gratitude to G. J. Hagood Jr., of the NASA Langley Research Center, for his vital assistance in setting up and operating the apparatus for conducting the vibration test program.

* Aerospace Technologist, Loads Division. Member AIAA.
† Mathematician, Loads Divsiion.

The model dimensions and eccentricities are indicated in Fig. 1 along with the material properties E, μ, and ρ.

Model End Conditions

Vibration tests were conducted on each model oriented vertically with the upper end free and the lower end fixed (or clamped) in an end plate as shown in Figs. 1 and 2. The end fixity was achieved by first aligning the lower end of the shell in an annular groove cut in the end plate. Ring sections fastened to the end plate along the inside edge of the groove provided temporary support for the shell and maintained its circular or elliptical cross section while the clamping action was being established. The groove was then filled with a low-melting-point, high-density potting material. Small spacers had previously been set in the bottom of the groove so that a little over $\frac{1}{2}$-in. of shell length was immersed in the potting material. The free length L above the top of the groove is given in Fig. 1 for each model. After the potting material solidified to establish the clamping action, the inner supporting ring fixtures were removed. Each model had its own annular groove and end plate.

Test Apparatus and Procedure

The essential parts of the test apparatus consisted of two types of vibration exciters, a noncontact inductance-type proximity sensor (or probe), a motorized trolley, and a movable supporting structure for the probe and trolley. The system comprising the exciters, probe, and trolley, together with the supporting instrumentation, is described in detail in Ref. 12.

Model excitation

The models were each excited by an oscillatory force directed normal to the shell surface and, throughout the test program, a small electrodynamic shaker was used for one of the vibration exciters. This shaker, which had a maximum vector force output of $1\frac{1}{2}$ lb, was suspended at the end of a soft spring and string combination and was attached to the inner shell surface by means of a lightweight vacuum-cup fastener.

The other vibration exciter used in the test program was an air shaker of the type described in Ref. 13. This shaker was used in some of the tests as an alternative means of excitation to verify certain results obtained with the electrodynamic shaker. The air shaker has the advantage of providing a noncontact exciting force permitting unrestricted motion of the shell wall and is therefore believed to give more reliable lower frequencies than the electrodynamic shaker, which can introduce unwanted stiffness and mass effects.[14] However, the frequencies covered in the test program were not low enough for the mass or stiffness of the electrodynamic shaker to significantly affect the frequencies of the model and, thus, more extensive testing by the air shaker was not considered necessary.

Model No.	a in.	b in.	$\frac{a}{b}$	e	L in.
1	12.00	12.00	1.00	0	23.422
2	12.95	11.01	1.176	0.526	23.438
3	14.39	9.35	1.538	0.760	23.440
4	16.39	6.56	2.50	0.916	23.400

$E = 10^7$ lb./ in.^{2}
$\mu = 0.3$
$\rho = 2.588 \times 10^{-4}$ $\frac{\text{lb.sec}^2}{\text{in.}^4}$

$e = \sqrt{1 - \left(\frac{b}{a}\right)^2}$

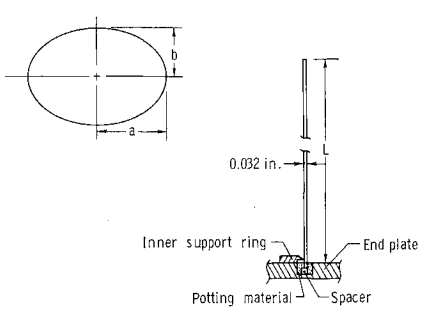

Fig. 1 Properties of clamped-free cylindrical shells.

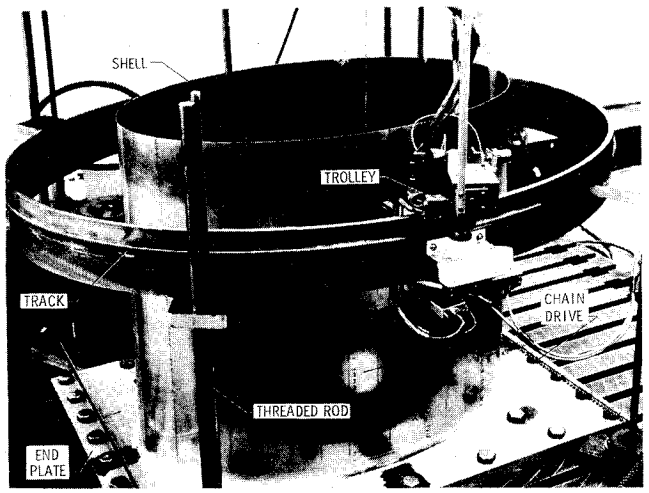

Fig. 2 View of apparatus for clamped-free elliptical cylindrical shell.

Mode shape measurements

Vibratory measurements of the shell wall in a direction normal to its surface were detected and recorded by means of a noncontact, inductance-type proximity sensor and its instrumentation. This device was mounted on a motorized trolley which ran on a track around the model, as shown in Figs. 2 and 3 for one of the elliptical shells. The track was, in turn, mounted on a support surrounding the model and capable of motorized movement vertically along the length of the model. For each elliptical shell, this support consisted of a $\frac{3}{8}$-in.-thick steel concentric strap mounted on four vertical threaded rods located near the corners of the end plate as shown in Fig. 2. These rods were rotated simultaneously by an electric motor supplying power to a chain drive and sprocket assembly visible on the heavy bed plate in Fig. 2. As the rods rotated, the concentric strap with the probe and trolley was raised or lowered in the axial direction of the model.

A detailed view of the probe and trolley assembly between the track support and the model is shown in Fig. 3. The thin white wire leading upward from the back of the probe itself leads to the electronic instrumentation which controls the distance of the probe from the model as well as the operation of a plotter that traces out normal shell displacements as the probe travels over the shell surface.

Test procedure

The general test procedure was as follows: 1) the exciting frequency was slowly increased until a resonance was found with the aid of Lissajous patterns on an oscilloscope and a maximum response was indicated on the instrumentation, 2) the inductance probe was then moved around the model to obtain the circumferential mode shapes at various vertical positions on the model, 3) the probe and its circumferential support were next moved vertically to determine the longitudinal mode shape, and 4) the resonant frequency of the model was read on an electronic counter which sampled the probe output for comparison with the shaker output.

Experimental Results

Resonant frequencies of vibration for the four clamped-free cylindrical shells are listed in Tables 1–4. Frequencies identified with (A) were obtained by use of the air shaker and are generally lower than those obtained with the electrody-

Table 1 Experimental and analytical frequencies of clamped-free cylindrical shells; circular shell: $a/b = 1.0, e = 0$

	$m = 1$		$m = 2$	
n	Exp.	Anal.	Exp.	Anal.
0		>2300 Hz		>2300 Hz
1		791.6		>2000
2		395.9		1314
3	201.8 Hz			
		219.3		876.8
	206.2			
4	131.7	138.2		613.6
5	100.8	103.3	429.1 Hz	449.7
6			[a]326.3	
	96.9	97.9		346.3
			[a]334.4	
7	113.0	112.1	273.5	283.8
8	140.4	138.1	247.4	252.6
9	174.3	171.3	244.2	246.8
10	214.6	210.1	261.5	260.9
11	258.4	253.7	292.1	289.6
12	307.6	301.7	335.2	328.8
13			381.1	
	361.2	354.1		375.8
			[c]393.2	
14	[a]416.0			
		410.8	437.8	429.1
	[b]424.9			

[a] Coupled with $n = 12$.
[b] Coupled with $n = 5$; strong localized shaker effect.
[c] Appears to be coupled with $m = 3$.

namic shaker. Differences in frequency between the two types of shakers are larger at lower frequencies than at higher ones but amounted to no more than about 6% (see $m = 1, p = 5$ and 6 in Table 3 and $m = 1, p = 5$ in Table 4).

The frequencies in Tables 1–4 are classified as shown in Fig. 4 by specifying integers m and p, where m is the longitudinal mode number and p is one-half the number of longitudinal nodes for an elliptical shell. For the circular shell, the integer n replaces p to denote the number of circumferential waves. Elliptical-shell frequencies are further classified as symmetric or antisymmetric according to a predominantly symmetric or antisymmetric normal-displacement response with respect to the minor axis.

The number of elliptical-shell resonances and corresponding mode shapes identified according to Fig. 4 decreased as eccentricity (e) increased. In some of these cases, different mode numbers p and m were observed in different parts of the model for a particular resonance. Moreover, a considerable number of modes had mixed symmetric and antisymmetric response characteristics, so that their classification according to Fig. 4 became somewhat arbitrary. Sample mode shapes, including those with these features, are presented in Figs. 5–8 for comparison with analytical mode shapes. Modes that were difficult to identify are noted in the footnotes of Tables 1–4.

Method of Analysis

Analytical frequencies and mode shapes were calculated by application of the modal vibration analysis described in Ref. 11 which is based on the well-known Rayleigh-Ritz procedure and Sander's thin-shell theory.[15] The deformation of the shell middle surface is expressed in terms of the in-plane and radial, or normal (N), displacements u, v, and w shown in Fig. 5. These displacements are each assumed to be the following finite series of products of circumferential and longitudinal modal functions for sinusoidal motion of frequency ω:

$$u(x,\theta,t) = \sum_{m=1}^{P} \sum_{p=0}^{Q} (\bar{a}_{mp} \cos p\theta + a_{mp} \sin p\theta) X_{mu}(x) e^{i\omega t} \quad (1a)$$

Table 2 Experimental and analytical frequencies of clamped-free cylindrical shells; elliptical shell: $a/b = 1.176, e = 0.526$

	$m = 1$				$m = 2$			
	Experiment		Analysis		Experiment		Analysis	
p	Sym.	Antisym.	Sym.	Antisym.	Sym.	Antisym.	Sym.	Antisym.
0			2656 Hz				2772 Hz	
1			739.2	840.1 Hz			1870	2181 Hz
2			390.6	394.1			1301	1332
								1347
3	201.9 Hz	204.8 Hz	217.5	217.5			881.0	884.4
	201.1 (A)							
4	129.5	134.0	136.4				616.0	616.0
	129.1 (A)							
5	96.4	100.2	99.45	99.45	[a]416.4 Hz	[a]433.9 Hz	450.9	450.9
6	94.2	94.5	95.9	95.9	327.3	328.4	347.6	347.6
	93.1 (A)							
7	115.1	116.5	114.2	114.2	281.6	276.9	282.3	
8	141.8	142.3	139.6	136.4	[b]224.6	237.4	238.9	238.9
	140.6 (A)			139.6	228.0			
9	176.0	176.2	171.4	171.4	228.7	235.5	237.3	237.3
								282.3
10	217.2	216.3	210.1	210.1	270.5	270.5	267.8	267.8
	217.1 (A)							
11	260.4	260.8	253.7	253.7	296.5	298.4	295.3	295.3
12	309.5	310.6	301.7	301.7	338.6		329.7	329.7
					[c]348.0			
13	365.0		354.1	354.1	[d]377.3	[e]374.8	376.2	376.2
					[d]383.5			
					[d]385.9			
14	423.6		410.7	410.7	443.6	[f]442.5	429.3	429.3

[a] Coupled with $p = 13$ (symmetric) and $p = 12$.
[b] Possibly coupled with $p = 9$ and 10.
[c] Coupled with $m = 3, p = 13$.
[d] Highly coupled with $m = 3, p = 12$.
[e] Coupled with $m = 3, p = 12$.
[f] Coupled with $p = 11, 12$.

Table 3 Experimental and analytical frequencies of clamped-free cylindrical shells; elliptical shell: $a/b = 1.538$, $e = 0.760$

	$m = 1$				$m = 2$			
	Experiment		Analysis		Experiment		Analysis	
p	Sym.	Antisym.	Sym.	Antisym.	Sym.	Antisym.	Sym.	Antisym.
0			2645 Hz				2898 Hz	
1			643.9	927.0 Hz				2909 Hz
2			357.2	378.8				1308
3	[a]195.2 Hz	[a]190.0 Hz	205.7	205.4			821.1	818.7
4		[b]117.4	126.3				582.6	583.8
		[b]121.5						
5	[c]87.8	[c]87.7	87.2	87.2			431.2	431.3
	[c]89.5							
6	[c]83.4 (A)		86.5	86.5			348.7	
	[c]85.5 (A)			126.4				
7	111.2	112.1	114.6	114.6				
	110.1 (A)	111.6 (A)						
8	143.0	140.8	143.1	143.1			205.7	205.7
	142.1 (A)	140.0 (A)						
9	170.4	168.6	170.9	170.9	[d]199.8 Hz	203.9 Hz	205.9	205.9
							258.5	258.5
10						244.5		
		208.8	209.9	209.9		246.9	255.8	255.8
11	251.8		253.0	253.0	[e]297.1	289.9	302.4	302.4
12			301.1	301.1	[e]310.0		319.2	319.2
						[f]338.4		348.8
13	351.8		353.6	353.6	370.2		377.8	377.8
14			412.0	412.0			432.8	432.9

[a] Possibly coupled with $p = 8$.
[b] Coupled with $p = 5$ and 6; have some symmetric characteristics.
[c] Highly coupled involving both $p = 5$ and $p = 6$.
[d] Involves some coupling with $m = 1$.
[e] Coupled with $p = 10$.
Coupled with $m = 3$, $p = 11$.

Table 4 Experimental and analytical frequencies of clamped-free cylindrical shells; elliptical shell: $a/b = 2.50$, $e = 0.916$

	$m = 1$				$m = 2$			
	Experiment		Analysis		Experiment		Analysis	
p	Sym.	Antisym.	Sym.	Antisym.	Sym.	Antisym.	Sym.	Antisym.
0			2646 Hz					
1				5083 Hz			1363 Hz	3572 Hz
2			263.8				834.4	1269
3				1033				
4				337.4				
5	59.8 Hz (A)	63.7 Hz	67.1	67.0				712.1
	62.7							
6	67.2	65.9 (A)	68.5	68.55				505.8
	69.0							
6	97.7	93.7 (A)	101.3	101.6		[b]142.0 Hz		
		94.7				151.6 (A)		
7	102.7	98.9	102.5	102.6		[c]140.8 (A)	672.0	
	103.4			153.3		[c]142.7		
						[c]146.2		
8	134.7		137.6	137.6	[b]137.7		159.1	159.1
	136.5 (A)				[b]139.3 (A)		495.4	
9	175.7	172.7	154.6	177.9	[d]192.7		159.5	159.5
	[a]176.8		179.5				209.7	209.8
10	[a]207.1		205.8	205.9		[e]203.2 (A)	211.5	211.5
							270.3	268.9
11			250.7	250.7		[f]245.8	270.5	270.5
						[f]346.9		342.6
12	298.4		298.9	296.0			332.2	328.2
13			350.6	350.6			342.4	398.4
							397.7	
14			407.3	407.8			423.5	424.5

[a] Strong localized shaker effect.
[b] Coupled with $m = 1$, $p = 7$.
[c] Coupled with $m = 1$, $p = 5$.
[d] Coupled with $p = 7$, 8.
[e] Coupled with $p = 8$.
Coupled with $m = 1$, $p = 10$.

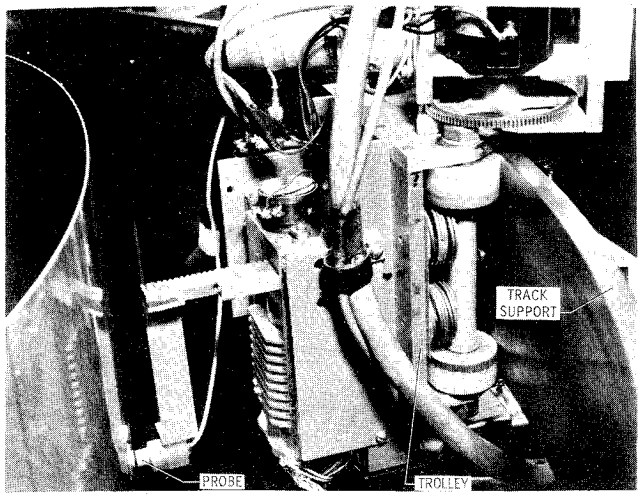

Fig. 3 Closeup of noncontact inductance probe and trolley.

$$v(x,\theta,t) = \sum_{m=1}^{P}\sum_{p=0}^{Q}(\bar{b}_{mp}\sin p\theta - b_{mp}\cos p\theta)X_{mv}(x)e^{i\omega t} \quad (1b)$$

$$w(x,\theta,t) = \sum_{m=1}^{P}\sum_{p=0}^{Q}(\bar{c}_{mp}\cos p\theta + c_{mp}\sin p\theta)X_{mw}(x)e^{i\omega t} \quad (1c)$$

where $\bar{a}_{mp}\ldots c_{mp}$ are amplitude coefficients (or generalized coordinates), the barred coefficients denoting symmetric terms and the unbarred coefficients anti-symmetric terms. The integers P and Q denote upper and lower limits of the longitudinal and circumferential modal series, respectively. The X_m terms represent longitudinal modal components which are chosen to approximate the longitudinal mode shapes and to satisfy prescribed displacement and slope conditions at the ends of the shell. For a clamped-free cylindrical shell, these terms may be approximated by

$$X_{mu} = X_m' \quad (2a)$$

$$X_{mv} = X_{mw} = X_m = \cosh N_m x - \cos N_m x - \gamma_m(\sinh B_m x - \sin N_m x) \quad (2b)$$

where $X_m' = dX_m/dx$ and N_m, γ_m are eigenvalue properties for a vibrating cantilever beam, as tabulated in Ref. 16, for example. These may be introduced into the analysis with the aid of the evaluated integrals for cantilever beams given in Ref. 17.

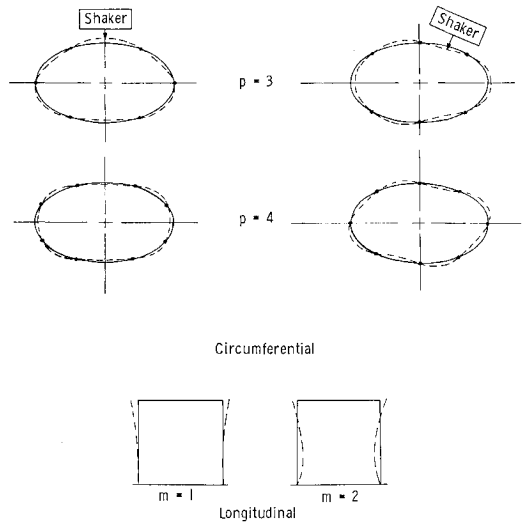

Fig. 4 Mode-shape classifications for normal (w) displacements.

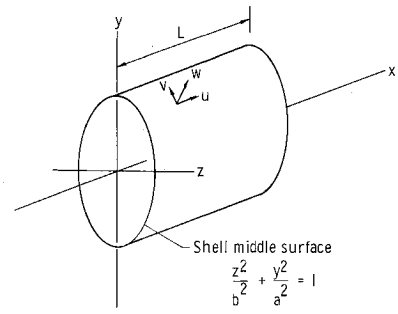

Fig. 5 Elliptical shell geometry.

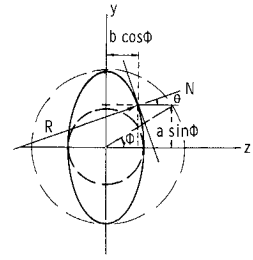

The displacements and slopes at the free end and the conditions $u = v = w = \partial w/\partial x = 0$ at the clamped end are satisfied by Eqs. (2). However, there is a contradiction of having both $v = 0$ and the in-plane shear stress resultant

$$N_{xy} = [Eh/2(1+\mu)](\partial u/\partial y + \partial v/\partial x) = 0$$

at the clamped end. The effects of this inconsistency were evaluated for the circular shell by choosing other longitudinal modal functions, and results indicate no more than a 3% increase in frequency (at $m = 2$, $n = 2$) and a negligible effect on both normal and in-plane mode shapes due to the use of Eqs. (2) in the analysis.

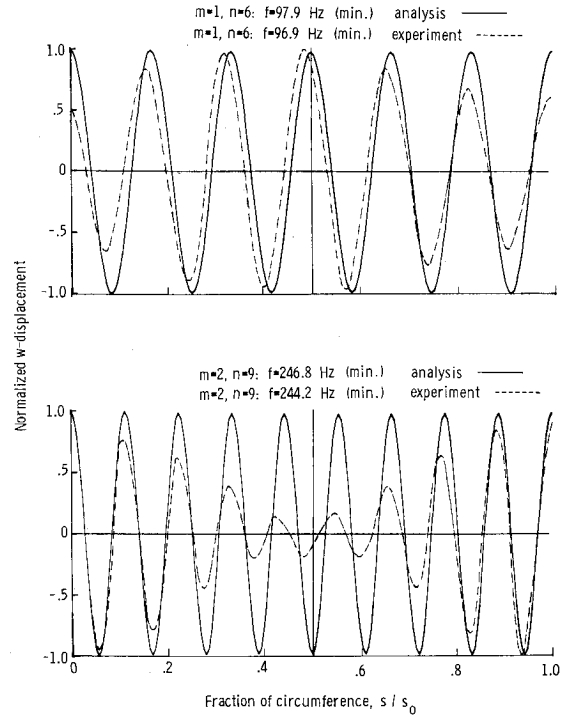

Fig. 6 Experimental and analytical circumferential mode shapes of clamped-free circular cylindrical shell (a/b = 1.0, e = 0).

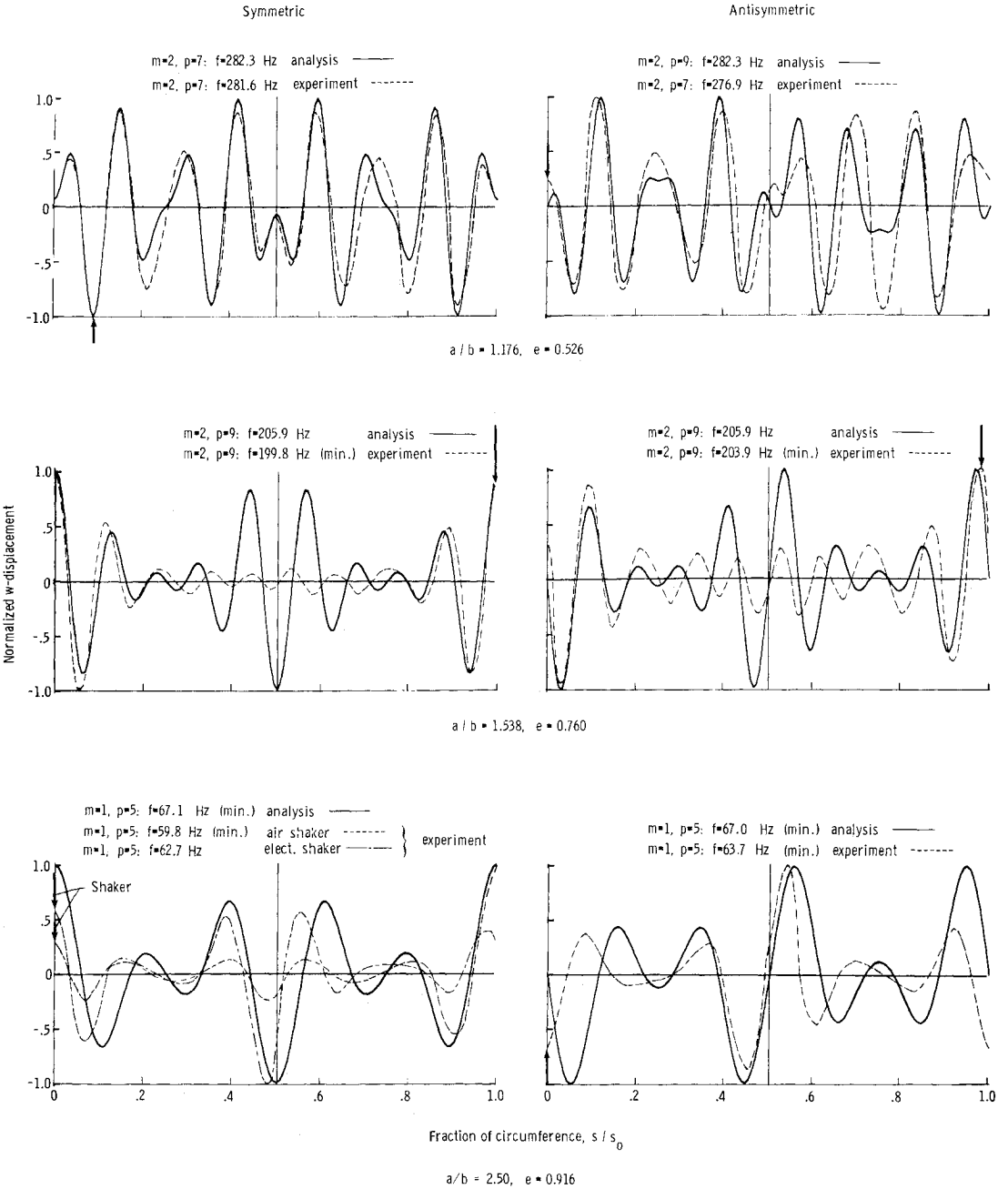

Fig. 7 Experimental and analytical circumferential mode shapes of clamped-free elliptical cylindrical shells.

Analytical Results and Comparison with Experiment

Analytical frequencies of the shells of Fig. 1 are listed in Tables 1–4 along with experimental frequencies, and generally good agreement between analytical and experimental frequencies is shown. Analytical mode shapes are compared with experimental mode shapes in Figs. 6–9, with Figs. 6 and 7 showing somewhat better agreement between analytical and experimental nodes than mode shapes for the circumferential modes. The generally good agreement between longitudinal analytical and experimental mode shapes indicates the validity of choosing beam functions for the longitudinal displacement terms in the series of Eqs. (1).

Convergence of Analytical Results

Analytical results in Tables 1–4 were considered converged with the inclusion of the number of terms in the series noted below. Beginning with the circular shell (model 1), which requires only a single circumferential term in each series, converged solutions for this model were obtained with four beam-function terms in each longitudinal displacement series. (The circular-shell results in Table 1, and Figs. 6 and 8 are actually based on five longitudinal modal functions.) Next, with this same number of longitudinal functions, the number of circumferential terms was increased to achieve convergence for each of the elliptical shells, and more of these circumferential terms were required with increasing eccentricity. Thus, 13 circumferential terms were needed for $e = 0.526$, 16 terms for $e = 0.760$, and at least 32 terms for $e = 0.916$ (model 4). At $e = 0.916$, the number of required terms exceeded the capacity of the computing facility (NASA Langley CDC 6600 Digital Computer). Hence, the number of longitudinal terms had to be reduced from 4 to 2 to allow for more circumferential terms, and the combination of two longitudinal and 32 circumferential functions gave results that are as close to convergence as could be obtained for this model. The number of circumferential terms required for convergence for each model applies to all even- or all odd-numbered functions in the displacement series of Eqs. (1). Even and odd trigono-

metric functions together in the same series uncouple from each other when introduced into the frequency equation.

Tables 2–4 show dual analytical frequencies for some mode numbers and no frequencies for others. There appears to be no consistency to this behavior other than the increasing number of such modes with increasing eccentricity. Calculations (not included) also show these dual modes to be sensitive to variations in the number of circumferential terms included in the displacement series, particularly for the highest eccentricity ($e = 0.916$). Moreover, in some cases, identical analytical frequencies were obtained for symmetric and antisymmetric modes with different p-numbers. This is illustrated in Fig. 7 for the pair of analytical mode shapes associated with $e = 0.526$, which have different values of p but the same frequency, 282.3 Hz. The similarity between analytical and experimental antisymmetric mode shapes should also be noted in this case.

Effects of Eccentricity

Experimental and analytical frequencies of both circular and elliptical shells generally followed similar trends, as evidenced in Fig. 10 as well as in Tables 1–4. Because of the analytical dual-frequency behavior, plots of the type shown in Fig. 10 were considered impracticable for eccentricities greater than $e = 0.526$. Agreement between experimental and analytical frequencies is better at lower eccentricities than at higher ones, and the generally excellent agreement for the circular-shell frequencies afforded a satisfactory basis for evaluating eccentricity effects of the elliptical shells.

Eccentricity effects on both experimental and analytical frequencies are summarized in Fig. 11. The variations shown are for minimum frequencies belonging to the longitudinal modal families $m = 1$ and 2, and these frequencies clearly decrease as eccentricity increases. With the greatest effect occurring for $e > 0.76$, the frequencies at $e = 0.916$ are about 38% lower than the circular-shell minimum frequencies for $m = 1$ and 44% lower for $m = 2$. Circumferential mode numbers p associated with these minimum frequencies are indicated adjacent to the curves and tend to decrease with increasing eccentricity. Frequency reductions with increasing eccentricity were also obtained for modes in the vicinity of the minimum frequencies, as is evident in a comparison among the four tables. Frequencies of modes with higher values of p were essentially unaffected by eccentricity.

Comparison of symmetric and antisymmetric frequencies in Tables 2–4 indicates a tendency toward increased separation of these two sets of frequencies with increased eccentricity. The separation in experimental frequencies was larger than the separation in analytical frequencies but was no more than about 2% for modes that could be clearly identified according to Fig. 4.

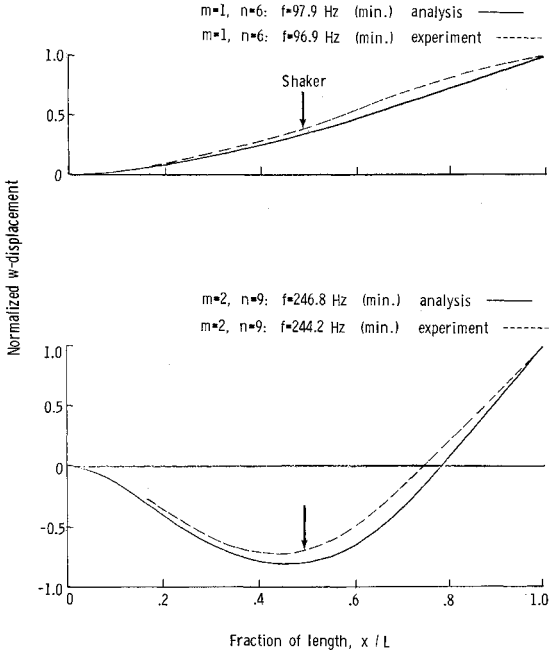

Fig. 8 Experimental and analytical longitudinal mode shapes of clamped-free circular cylindrical shell ($a/b = 1.0, e = 0$).

Concluding Remarks

Natural frequencies and associated mode shapes of a family of clamped-free elliptical cylindrical shells of constant mass are compared with analytical frequencies and mode shapes calculated by means of a Rayleigh-Ritz type of analysis featuring multiterm circumferential and longitudinal modal expansions. Vibration tests were conducted on four short thin-shell isotropic cylinders ranging in eccentricity

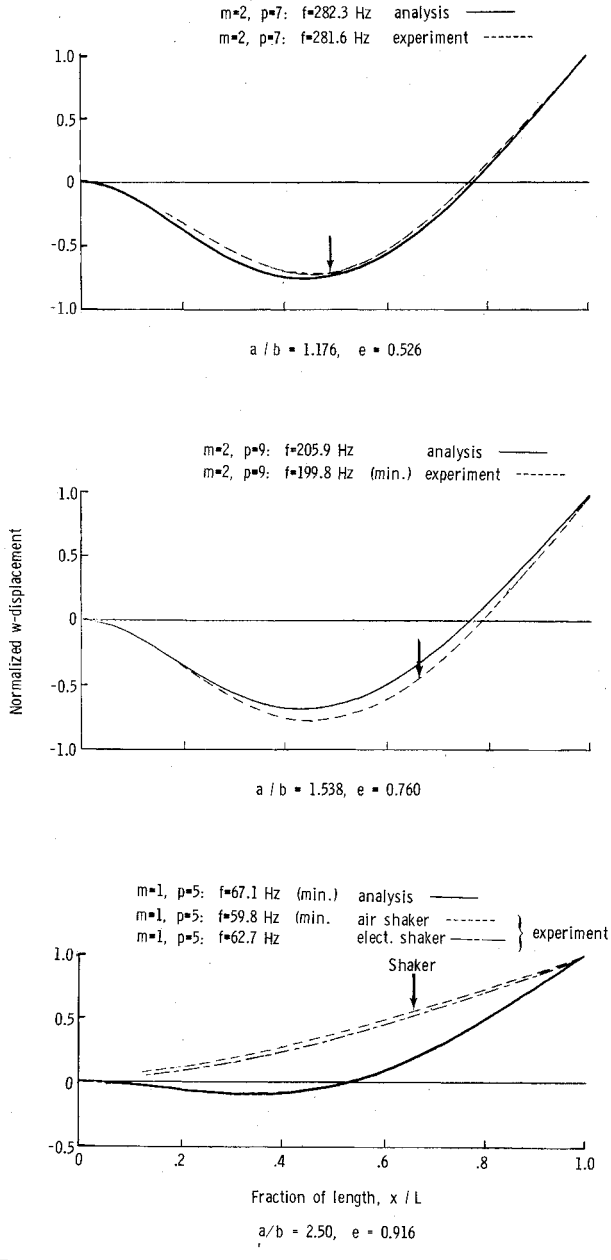

Fig. 9 Experimental and analytical longitudinal mode shapes of clamped-free elliptical cylindrical shells.

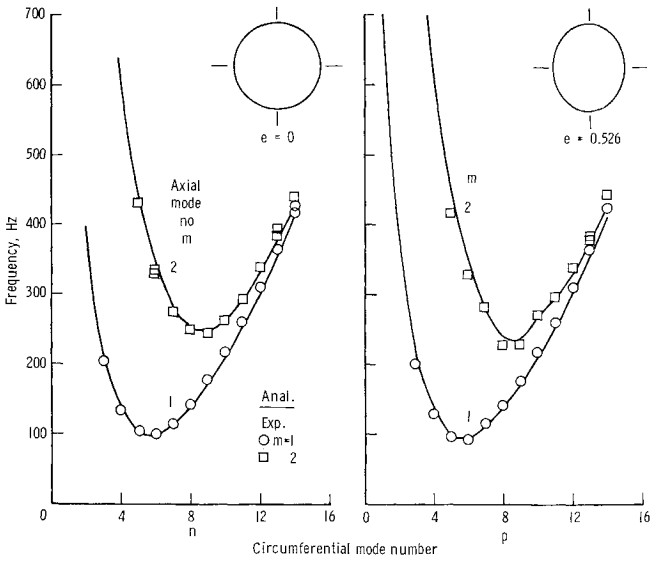

Fig. 10 Variation of frequencies with mode numbers.

from zero (circular cylinder) to 0.916. Mode shapes were measured by means of a noncontact inductance-type proximity sensor that could be moved over most of the surface of the model to obtain circumferential and longitudinal mode shapes.

Experimental results are in generally good agreement with analytical results, and both show reductions in frequency by as much as 44% due to increasing eccentricity from zero to 0.916. Four beam-type longitudinal functions and an increasing number of trigonometric circumferential functions were required to obtain converged analytical results with increasing eccentricity. As many as 32 circumferential terms were required for the highest eccentricity of 0.916.

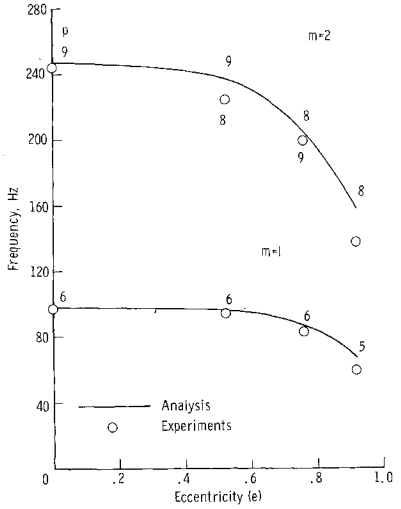

Fig. 11 Effects of eccentricity on minimum frequencies.

References

[1] Herrmann, G. and Mirsky, I., "On Vibrations of Cylindrical Shells of Elliptic Cross Section," Contract AF18(600)-1247, TN 5, Dec. 1957, Dept. of Civil Engineering and Engineering Mechanics, Institute of Flight Structures, Columbia Univ.

[2] Klosner, J. M. and Pohle, F. V., "Natural Frequencies of an Infinitely Long Noncircular Cylindrical Shell—Part I," PIBAL Rept. 476, Contract Nowr 839(17), July 1958, Dept. of Aeronautical Engineering and Applied Mechanics, Polytechnic Institute of Brooklyn.

[3] Klosner, J., "Frequencies of an Infinitely Long Noncircular Shell, Part II—Plane Strain, Torsional, and Flexural Modes," PIBAL Rept. 552, Contract Nowr 839(17), Dec. 1959, Dept. of Aeronautical Engineering and Applied Mechanics, Polytechnic Institute of Brooklyn.

[4] Klosner, J., "Free and Forced Vibrations of a Long Noncircular Cylindrical Shell," PIBAL Rept. 561, Contract Nowr 839(17), Sept. 1960, Dept. of Aeronautical Engineering and Applied Mechanics, Polytechnic Institute of Brooklyn.

[5] Malkina, R. L., "Vibrations of Noncircular Cylindrical Shells," *Izvestiya Akademiia Nauk SSSR, Otdelenie Tekhnicheskikh Nauk, Mekhanika i Mashinostroenie*, No. 1, 1960, pp. 172–175; translation Lockheed Missiles & Space Co.

[6] Slepov, B. I., "Vibrations and Stability of an Elliptical Shell," *Izvestiya Akademii Nauk SSSR, Mekhanika i Mashinostroenie*, No. 3, 1964, pp. 144–146; translation TT F-12,155, March 1969, NASA.

[7] Kozarov, M., "Stability and Dynamics of Orthotropic Elliptically Cylindrical Shells," *Izvestiya na Ynstituta po Teklnycheska Mekhanika*, Vol. 1, pp. 149–157; translation TT F-12,197, May 1969, NASA.

[8] Ivanyuta, E. I. and Finkel'shteyn, R. M., "Determination of the Free Oscillations of a Cylindrical Shell of Elliptical Cross-Section," *Issledovaniya po uprugosti i plastichvosti*, Vol. 1, 1964, pp. 46–51; translation TT F-12,548 Aug. 1969, NASA.

[9] Park, A. C. et al., "Dynamics of Shell-Like Lifting Bodies, Part II—Experimental Investigation," TR AFFDL-TR-65-17, Pt. II, June 1965, North American Aviation Inc.

[10] Sal'nikov, G. M. and Zenukov, A. G., "Determination of the Natural Oscillating Frequencies of Shells of Complex Shape With Free Edges," *Izvestiya Vysshikh Uchebnykh Zavedeniy, Seriya, "Aviatsionnaia Tekhnika,"* Vol. 10, No. 4, 1967, pp. 143–148; translation TT F-11,719, May 1968, NASA.

[11] Sewall, J. L., Thompson, W. M., Jr., and Pusey, C. G., "An Experimental and Analytical Vibration Study of Elliptical Cylindrical Shells," TN D-6089, Feb. 1971, NASA.

[12] Naumann, E. C. and Flagge, B., "A Noncontacting Displacement Measuring Technique and Its Application to Current Vibration Testing," Preprint 16.18-5-66, Oct. 1966, Instrument Society of America.

[13] Herr, R. W., "A Wide-Frequency Range Air Jet Shaker," TN 4060, 1957, NACA.

[14] Mixson, J. S., "Experimental Modes of Vibration of 14° Conical-Frustum Shells With Free Ends," TN D-4428, 1968, NASA.

[15] Sanders, J. L., Jr., "An Improved First-Approximation Theory for Thin Shells," TR R-24, 1959, NASA.

[16] Young, D. and Felgar, R. P., Jr., "Tables of Characteristic Functions Representing Normal Modes of Vibration of a Beam," Publication 4913, Engineering Research Series 44, July 1, 1949, Bureau of Engineering Research, Univ. of Texas.

[17] Felgar, R. P., Jr., "Formulas for Integrals Containing Characteristic Functions of a Vibrating Beam," Circular 14, 1950, Bureau of Engineering Research, Univ. of Texas.